https://doi.org/10.1016/j.ijepes.2020.106411

Short-term Prediction of Wind Power and Its Ramp Events based on Semi-supervised Generative Adversarial Network

Bin Zhou[a*], Haoran Duan[a], Qiuwei Wu[b], Huaizhi Wang[c*], Siu Wing Or[d,e*], Ka Wing Chan[d], Yunfan Meng[a]

[a]*College of Electrical and Information Engineering, Hunan University, Changsha 410082, China*
[b]*Department of Electrical Engineering, Technical University of Denmark, Lyngby 2800, Denmark*
[c]*Guangdong Key Laboratory of Electromagnetic Control and Intelligent Robots, Shenzhen University, Shenzhen 518060, China*
[d]*Department of Electrical Engineering, The Hong Kong Polytechnic University, Hung Hom, Kowloon, Hong Kong*
[e]*Hong Kong Branch of National Rail Transit Electrification and Automation Engineering Technology Research Center, Hong Kong.*

Abstract: Short-term predictions of wind power and its ramp events play a critical role in economic operation and risk management of smart grid. This paper proposes a hybrid forecasting model based on semi-supervised generative adversarial network (GAN) to solve the short-term wind power outputs and ramp event forecasting problems. In the proposed model, the original time series of wind energy data can be decomposed into several sub-series characterized by intrinsic mode functions (IMFs) with different frequencies, and the semi-supervised regression with label learning is employed for data augmentation to extract non-linear and dynamic behaviors from each IMF. Then, the GAN generative model is used to obtain unlabeled virtual samples for capturing data distribution characteristics of wind power outputs, while the discriminative model is redesigned with a semi-supervised regression layer to perform the point prediction of wind power. These two GAN models form a min-max game so as to improve the sample generation quality and reduce forecasting errors. Moreover, a self-tuning forecasting strategy with multi-label classifier is proposed to facilitate the forecasting of wind power ramp events. Finally, the real data of a wind farm from Belgium is collected in the case study to demonstrate the superior performance of the proposed approach compared with other forecasting algorithms.

Highlights

Wind power prediction problem is formulated as a min-max game based on GAN.
Semi-supervised regression is used for the point prediction of wind power.
A double objective model is designed for data augmentation and feature extraction.
A self-tuning strategy is proposed for forecasting of wind power ramp events.

Keywords: Generative adversarial network; semi-supervised regression; wind power forecasting; wind power ramp event; renewable energy.

*E-mail addresses of corresponding authors: wanghz@szu.edu.cn (H. Wang), binzhou@hnu.edu.cn (B. Zhou), eeswor@polyu.edu.hk (S. W. Or).

1 Introduction

1.1 Motivation

As a clean, green and environmentally friendly renewable energy resource, wind energy has developed rapidly in recent years [1]. The penetration of wind energy poses significant challenges to the economic operation, reliability and real-time control of electrical power and energy system [2]. Statistics in [3] reported that global installation capacity of wind power has reached 597GW in 2018, with an increase of 9.1% over last year. Nevertheless, because of high volatility and intermittency of wind energy, especially for large and sudden ramp events, various energy storage systems and fast hydropower plants should be utilized as power reserves to mitigate the fluctuating wind generation outputs for real-time electricity supply demand balance [4]. Hence, developing accurate and reliable wind energy prediction techniques has become a common priority for the energy scheduling of dispatchable power sources to accommodate large-scale wind farms in power grids, thereby increasing wind energy's contribution to global electrical power supply [5]-[6].

Wind power ramp prediction is a challenging problem and has received great attentions in recent years, as large forecasting deviations of wind power or misidentification of ramp events would exacerbate the smart grid reliability and operations. The wind power ramp event is referred as a suddenly-increasing or decreasing fluctuation of wind power within a short-time period, and these events usually come from extreme atmospheric phenomena, such as thunderstorms, cyclones, wind gusts or low-level jets [7]. Wind power ramps can be divided into different types and characterized by their ramping direction, duration, and intensity. The basic types include ramp up and ramp down events. Pitch angle control of wind turbines or energy storage technology can be used to avoid the imbalance between power generation and load when a ramp up event occurs, thereby reducing wind energy curtailment. To address a ramp down event, system operators can regulate the power outputs of dispatchable generators and energy storage systems to compensate the power shortage caused by sudden wind power reductions [8]. Integrating high-penetration wind energy into smart grid urgently requires accurate wind energy prediction and ramp event identification [8]. Therefore, this paper aims to address the short-term prediction of wind power and its ramp events based on the advanced generative adversarial network.

1.2 Relevant Background

The researches on point prediction of wind power can be classified into three categories: physical methods, mathematical statistical methods, and machine learning algorithms [5]. Physical methods focus on establishing a mathematical relationship between meteorological, environmental and geographical

information and wind power outputs. The meteorological, environmental and geographical information are usually collected from numerical weather prediction (NWP) systems, including atmospheric pressure, temperature, wind direction, wind farm location and terrain [9]. A hybrid model combining NWP and Gaussian processes was proposed in [10] for short-term forecasting of wind energy, and the forecasting results of the hybrid approach was comprehensively tested. As NWP models often require a large amount of meteorological information and computing resources, physical methods are generally not applicable to short-term wind energy forecasting [4]. Statistical methods are developed to formulate a mathematical relationship between the historical wind power time-series and future forecasting values. Typical statistical methods include autoregressive integrated moving average model (ARIMA) [11], autoregressive model [12], Kalman filter (KF) [13]-[14], Bayesian learning [15], Gaussian process [10]. Fei *et al.* in [16] proposed a forecasting model combining empirical mode decomposition (EMD) and ARIMA, and the prediction performance in several simulation examples was tested. In [17], an adaptive hybrid model based on variational mode decomposition (VMD), ARIMA and deep neural network for wind speed forecasting was designed. ARIMA model was built to predict regular component decomposed by VMD. However, most of statistical methods are often modeled as simplified linear functions, so the prediction performance of statistical models may be largely limited.

Recently, various machine learning algorithms have been developed for wind energy forecasting. In order to address the classification, feature extraction and nonlinear regression problems in wind energy prediction, lots of machine learning techniques are presented [18]-[30]. Typical machine learning algorithms include support vector machine (SVM) [18], artificial neural network (ANN) [19]-[20], neuron-fuzzy network [21], extreme learning machine (ELM) [22]-[23], random vector functional link network (RVFLN) [24], recurrent neural network (RNN) [25], long short term memory network (LSTM) [26] and convolutional neural network (CNN) [27], The study in [27] and [28] designed two structures based on the deep CNN and deep belief network (DBN) to achieve the accurate forecasting of solar photovoltaic and wind power outputs, respectively. Extensive studies in [19]-[26] have demonstrated that the prediction models based on traditional backward propagation mechanism have several problems, such as over-fitting and be prone to local minimum. In order to solve these problems, heuristic optimization algorithms have been used, such as genetic algorithm and particle swarm optimizer [29]. In general, these machine learning-based models typically have better forecasting results than the physical and statistical methods due to their powerful feature learning capabilities [28]. Moreover, various signal decomposition techniques, such as wavelet transformation (WT) [27], wavelet packet decomposition (WPD) [26], EMD [16], ensemble empirical mode decomposition (EEMD), and VMD [20], have been used along with ANN, CNN, LSTM or other machine learning algorithms to cope with the wind power time series a variety of

irregularities [30].

Due to the intrinsic fluctuation and volatility of wind speed, the grid-connected wind power poses a great threat to the economic and secure operation of smart grid, especially when the wind speed undergoes a large ramp event. So far, wind power ramp forecasting methods can fall into two categories: indirect forecasting and direct forecasting methods [7]. In the direct methods, one or several parameters related to wind power ramp events, such as the ramp rate and duration, can be forecasted directly on the basis of historical ramp events. In [31], a data mining approach was proposed for the direct ramp event forecasting (REF), and a feature selection model based on mutual information was employed to optimize the SVM classifier inputs. In [32], a probabilistic model was proposed to provide a suitable uncertainty estimation associated with the forecasting of a ramp event based on the NWP information. Nevertheless, these direct methods may lead to a large prediction bias when historical ramp events are incomplete [8].

For the indirect methods, the deterministic point forecasting model of wind power is performed and then its ramp events can be extracted latterly [33]-[35]. An ANN network was established in [33] for the short-term wind power prediction under different operational scenarios, so as to extract wind power ramp statistics on the ramp swing, ramp start time and ramp duration. A feature mining technique was presented in [34] to predict wind power ramp events, and the competitive and robust performance within hourly forecasting horizon were validated with existing benchmarking methods. A hybrid indirect REF model based on support vector regression was discussed and assessed using various absolute error metrics in [35]. Besides, an optimized swing door algorithm based on dynamic programming was developed in [36] to improve the REF capability of wind power and reduce the missing rate of ramp events. Because of its superior forecasting accuracy and applicability [8], the indirect REF method is adopted with a self-tuning forecasting strategy in this study to solve the forecasting problem of wind power ramp events.

1.3 Contribution and Organization of this Paper

In this paper, a hybrid forecasting model is proposed based on generative adversarial network (GAN) and semi-supervised regression for the short-term forecasting of wind power and its ramp events. GAN algorithm has been highly concerned and extensively applied in the technical fields of image processing, scenario generation, and speech synthesis [37]. The GAN exhibits a strong generalization capability to generate virtual samples similar to real samples. In the proposed method, the semi-supervised regression with label learning is integrated into the GAN framework for data augmentation to extract intrinsic non-linear and dynamic behaviors from wind power time series, and the improved performance for point prediction of wind power can be obtained. The main contributions of this paper can be summarized as follows:

(1) The problem of wind power forecasting (WPF) is formulated as a min-max game based on the GAN framework. This formulation is utilized to extract the potential statistical distribution and features in the wind power time series from labeled samples and unlabeled virtual samples. Hence, the under-fitting problem in the traditional GAN training process can be solved.

(2) A hybrid point forecasting method based on the GAN and semi-supervised regression is proposed to address the WPF and REF problems. The improved GAN uses the generative model to expand the training samples, while the discriminative model with a semi-supervised regression layer is redesigned to minimize the dual-objective GAN function, thereby improving the prediction accuracy of wind power.

(3) A self-tuning forecasting strategy with rolling horizon procedures is proposed to adjust the REF results of wind power ramp events in the future horizons based on the updated real-time information. A multi-label classifier is further employed to analyze wind power ramp characteristics and assign multiple labels to different types of ramp events based on ramp rate and given thresholds. The self-tuning strategy with multi-label ramp event features can facilitate the semi-supervised GAN to improve the forecasting accuracy of wind power ramp events.

The feasibility and effectiveness of the proposed forecasting method are verified in real wind power from a wind farm in Belgium. The rest of this paper is organized as follows: Section 2 introduces the algorithm framework and models of the classic GAN. Sections 3 and 4 propose GAN-based WPF and self-tuning REF frameworks, respectively. Section 5 describes the overall implementation steps for GAN-based WPF and self-tuning REF approaches. Then, the overall indices for evaluating the forecasting performance are introduced in Section 6. Section 7 provides case studies and comparative analysis, and the conclusions is given in Section 8.

2 Generative Adversarial Network

As a typical unsupervised deep learning method, the GAN algorithm has been extensively used to solve the problems of image processing, feature extraction and model recognition [37]-[38] . In the GAN framework, the generative model and the discriminative model compete with each other to produce optimal forecasting results. This Section mainly presents the detailed structure of GAN algorithm and its calculation processes.

2.1 Algorithm Framework of GAN

Inspired by the zero-sum game, Goodfellow first proposed a GAN structure including a generative model and a discriminative model in 2014 [37]. The generative model is used to extract the potential complex distribution in real data samples and generate virtual samples, and the discriminative model is

used to identify whether the input comes from a real sample or a virtual sample. Generative model and discriminative model are continually optimized through min-max games to increase their ability to generate or discriminate. The basic architecture of the GAN is presented in Fig. 1. In this figure, *G* and *D* correspond to the generative model and discriminative model in the GAN, respectively.

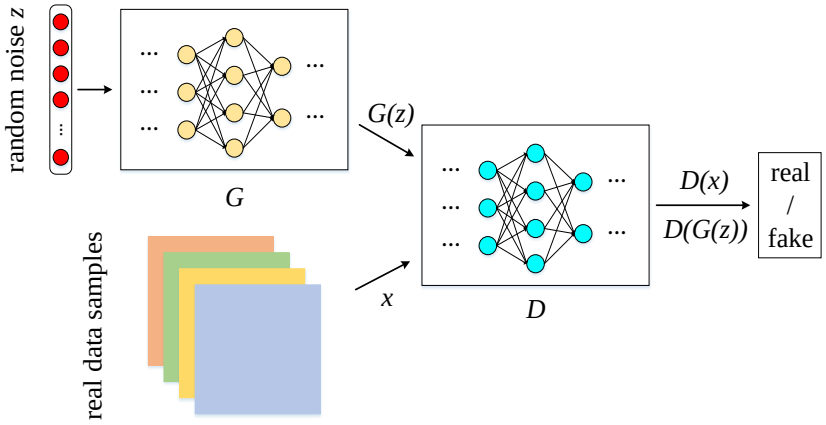

Fig. 1 Basic algorithm structure of GAN

As shown in Fig. 1, both the real sample $\boldsymbol{x}$ and the virtual sample $G(z)$ generated by the generative model can be used as the input to the discriminative model. If the input is $G(z)$, the output of the discriminative model is marked as "0". If the input is the real sample $\boldsymbol{x}$, the output of the discriminative model is marked as "1". It can be seen that the discriminative model is essentially a binary classifier. The main objective of generative model is to mimic the complex distribution of real sample data so as to achieve the purpose of deceiving the discriminative model. Thus, *G* and *D* are actually a dynamic game. In the most ideal state, *G* can generate a virtual sample $G(z)$, and it is hard for *D* to decide whether the virtual sample generated by *G* is true or not [38].

2.2 Min-Max Game of GAN Models

The objective function of the discriminative model is easy to define because its objective is relatively simple, that is, the output of discriminative model corresponds to 1 and 0 when the input is $\boldsymbol{x}$ and $G(z)$, respectively. In general, the training process of discriminative model minimizes the following objective function based on the cross entropy [38], as follows:

$$L_D = -\frac{1}{2}\mathrm{E}\cdot\log[D(x)] - \frac{1}{2}\mathrm{E}\cdot\log[1-D(G(z))] \tag{1}$$

where $\boldsymbol{x}$ and z represent real sample and random noise, respectively; E stands for an expectation.

The goal of the generative model is to mimic the complex distribution in real data by minimizing the objective function in Eq. (2), so as to achieve the purpose of making $D(G(z))$ close to 1:

$$L_G = \frac{1}{2}\mathrm{E}\cdot\log[1-D(G(z))] \tag{2}$$

It can be seen from Eq. (1)-(2) that L_D and L_G can constitute a dynamic min-max optimization game [39], as follows:

$$\min_G \max_D V(D,G) = \mathrm{E}\cdot\log[D(x)]+\mathrm{E}\cdot\log[1-D(G(z))] \tag{3}$$

In general, the generative model and discriminative model in the GAN are alternately optimized so that they can reach the stable state of Nash equilibrium [37].

3 GAN Based Wind Power Forecasting Approach

3.1 GAN Prediction Structure

The proposed prediction structure hybridizes different techniques for signal decomposition, sample generation, feature extraction and alternative training, as shown in Fig. 2. Firstly, the VMD is employed to decompose raw wind power time series into several intrinsic mode functions (IMFs). Then, the GAN generative model is used with linear layers, up-pooling layers and deconvolution layers to generate virtual wind power time series $\boldsymbol{P}_{\text{fake}}=\{P'_{t-s+1},P'_{t-s+2},\ldots,P'_t\}$ for capturing data distribution characteristics of wind power. Furthermore, the GAN discriminative model utilizes convolution and pooling operations to extract nonlinear features hidden in the wind power time series, and the semi-supervised regression is employed to forecast the wind power in the following horizons. Finally, an alternative training process is used to update parameters of GAN towards their optimal states for minimizing forecasting errors.

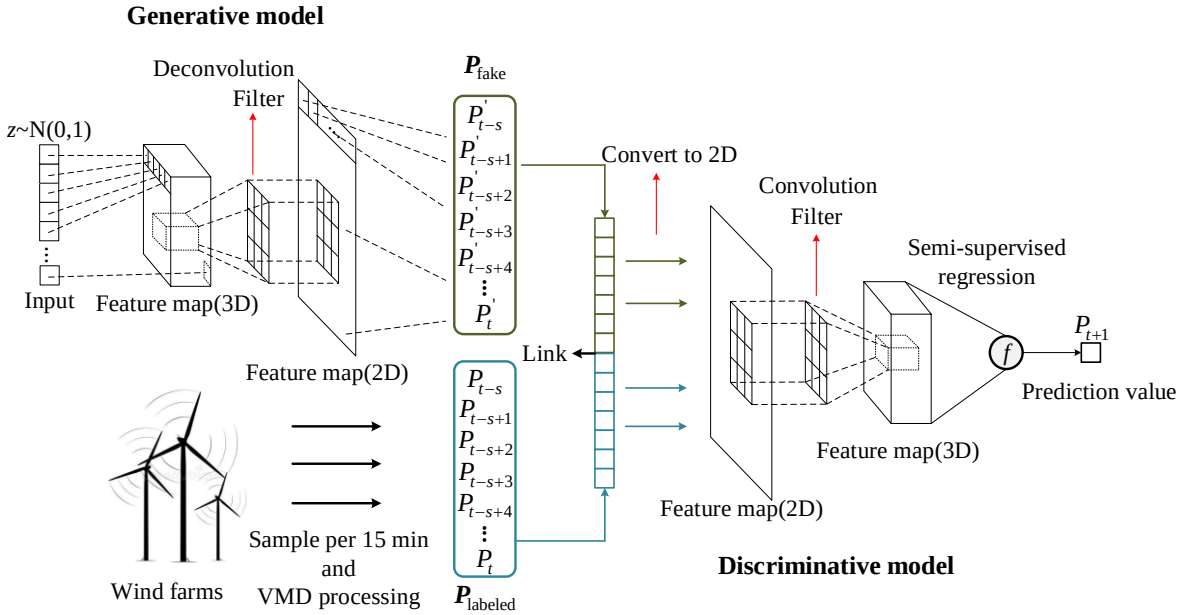

Fig. 2 The proposed semi-supervised regression GAN structure

3.2 Variational Mode Decomposition

Original wind power time series collected from real wind farms always exhibit strong nonlinearity

and irregular fluctuations. These features will degrade the accuracy of WPF and REF results. In this study, a VMD technique is adopted to decompose the original wind power time series into different variational modes u_k with limited bandwidth [17]. The VMD is an effective technique for the frequency domain decomposition of signals, especially for processing nonlinear and non-steady signals [17]. Different from the cyclic screening stripping used by EMD [16], the VMD can shift the signal decomposition process into variational modes so as to achieve the adaptive decomposition of wind power time series based on frequency domain characteristics of the decomposed signals, which is beneficial to reduce the impacts of data noise and outliers. Generally, these decomposed modes form a set $\{\boldsymbol{u_k}\} = \{u_1, u_2, \dots, u_k\}$ and each mode in the set can be defined as follows:

$$u_k(t) = A_k(t)\cos(\phi_k(t)) \tag{4}$$

where, $A_k(t)$ represents the instantaneous amplitude; $\phi_k(t)$ represents the instantaneous phrase; k is the number of modes.

There is a right number k of mode function corresponding to different original signals. In this study, the number of modes is set to 3 according to setting rules in [20]. Consequently, the original wind power series can be adaptively processed and decomposed into multiple sub-series with lower uncertainties based on the VMD. In the following, an independent GAN model for each sub-series will be developed to extract the inherent features of time series.

3.3 Sample Generation with Generative Model

Deep learning usually has a deep ANN structure with many model parameters, and massive training samples are required to make the algorithm converge. Nevertheless, collecting massive samples is very time consuming and expensive [30]. On the other hand, traditional sample generation techniques usually use uniform sampling, which is essentially the same as the original sample [38]. Therefore, a new sample generation technique is required to expand the training samples for enhancing the generalization ability of deep learning algorithms.

CNN algorithm is adopted in the generative model to obtain virtual samples, as the CNN has better feature extraction capability and less model parameters with the weight sharing technique. However, the CNN cannot be directly used for signal processing on the time series of wind power data and noise data because these time series data is usually one-dimensional. To this end, a data dimension conversion technique is adopted in this paper to solve this problem. In this way, the basic structure of GAN generative model can be described as follows: 1) Converting one-dimensional data samples into two-dimensional image samples, and taking the samples as the inputs to the convolution layer; 2) Mapping multiple low-dimensional images using several transposed convolution layers to the high-dimensional data space in

order to mimic the complex distribution of real samples; 3) Converting these two-dimensional image features into one-dimensional data to match the input dimension of the discriminative model; (4) Sending the virtual samples $\boldsymbol{P}_{\text{fake}}$ and real samples $\boldsymbol{P}_{\text{labeled}}$ to the GAN discriminative model. The multi-layer architecture of the generative model in the GAN is displayed in Fig. 3.

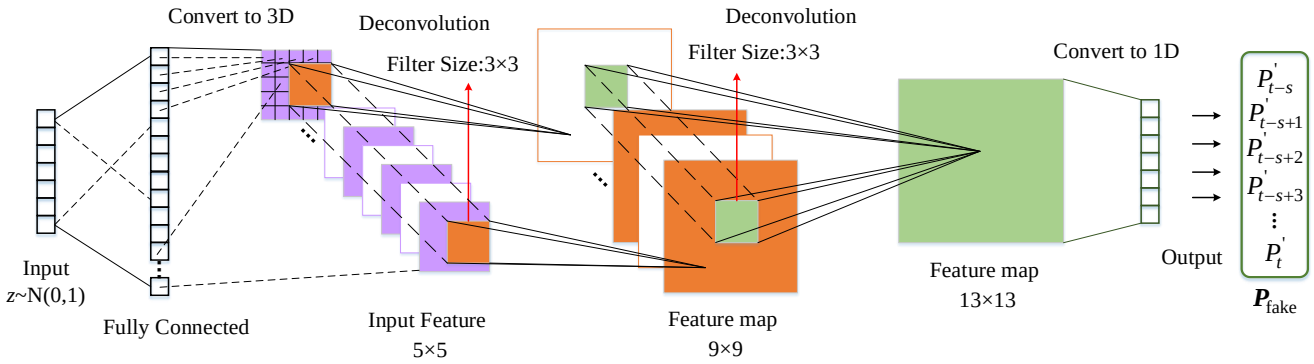

Fig. 3 Generative model architecture in the GAN

The primary objective of generative model is to mimic the complex distribution of real samples in an unsupervised manner. Therefore, the GAN generative model can generate a deceptive virtual sample according to the random noise [37]. The objective function of the unsupervised learning is expressed as:

$$L_G = \| E \cdot f(\boldsymbol{P}_{\text{fake}}) - E \cdot f(\boldsymbol{P}_{\text{labeled}}) \|^2 \tag{5}$$

where $f(\boldsymbol{P}_{\text{fake}})$ and $f(\boldsymbol{P}_{\text{labeled}})$ denote the output of an intermediate layer of the discriminative model; $\boldsymbol{P}_{\text{fake}}$ and $\boldsymbol{P}_{\text{labeled}}$ represent virtual wind power series and labeled wind power series, respectively.

By iteratively minimizing L_G in Eq. (5), the statistical features of the virtual samples and original samples tend to be more and more similar. These generated virtual samples can be viewed as an extension of the real samples, which can be utilized again to train the GAN model structure and parameters. Thus, the problem in wind power prediction scenarios, i.e., the training samples are limited, can be handled.

3.4 Feature Extraction with Discriminative Model

Furthermore, a modified discriminative model with semi-supervised regression [39] is proposed to form the nonlinear mathematical relationship functions between the historical time-series data and future prediction values of wind power. The modified discriminative model is illustrated in Fig. 4 and can be explained as: 1) Taking the virtual samples and the real wind power samples of wind power data as the inputs to the discriminative model; 2) Converting the inputs samples into a feature map; 3) Performing the convolution and pooling operations to obtain a high-dimensional characteristic representation of the input samples; 4) Finally, the regression layer is connected to the fully connected layer at the end of discriminative model to achieve nonlinear regression of the wind power data to obtain WPF results. It is worth noting that the outputs of the discriminative model is the prediction results of wind power, instead

of binary classification results in the basic GAN discriminative model.

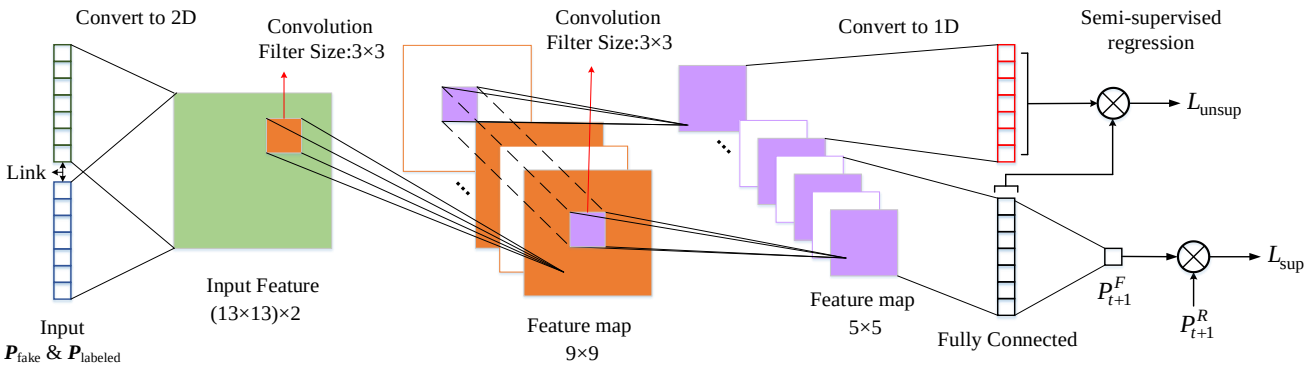

Fig. 4 Discriminative model architecture in the GAN

The proposed discriminative model includes a feature extraction layer and a regression layer. The feature extraction layer a uses an unsupervised learning technique while the regression layer performs with a supervised learning mechanism [5]. In order to enhance the regression capability of the developed discriminative model, a dual-objective optimization model is implemented with alternative training, and it can be expressed as follows,

$$L_{\mathrm{D}} = L_{\mathrm{unsup}} + L_{\mathrm{sup}} \tag{6}$$

$$L_{\mathrm{unsup}} = -\| E \cdot f(\boldsymbol{P}_{\mathrm{fake}}) - E \cdot f(\boldsymbol{P}_{\mathrm{labeled}}) \|^2 \tag{7}$$

$$L_{\mathrm{sup}} = E \cdot \left(P^F_{t+1} - P^R_{t+1} \right)^2 \tag{8}$$

where P^F_{t+1} and P^R_{t+1} represent the wind power prediction results and the real value at next time instant; $\boldsymbol{P}_{\mathrm{labeled}}$ and $\boldsymbol{P}_{\mathrm{fake}}$ indicate labeled wind power series and virtual wind power series, respectively.

It can be found that Eq. (7) is an unsupervised loss function to make the statistical distribution of virtual samples and real samples as dissimilar as possible. Eq. (8) is the supervised loss function, which is devoted to quantitatively assess the statistical deviations of the real wind power data as well as its predicted values. In other words, the regression minimization of loss function in (8) is the realization of the short-time prediction of wind power. It can be observed from Eq. (5) and Eq. (6) that the objective functions of GAN generative and discriminative models are competing to form a min-max game [39]. With the aid of virtual samples in the GAN generative model, the discriminative model can more readily to find the potential features in the original wind power samples, making the GAN predictions closer to their true values. Up to date, the alternative training process is generally used for well-training of the GAN, as detailed in the next Section.

3.5 Alternative Training Process

The GAN usually uses an alternative training method [37] to form a min-max game between GAN generative and discriminative models, thereby iteratively updating the model parameters of the GAN. In

this paper, an alternative training with adaptive moment estimation optimizer is applied to train the whole network of GAN. The training steps are given as follows:

Step 1: A set of noise vectors is generated and used as the input to the generative model, thereby obtaining a set of generated virtual samples;

Step 2: The virtual samples and their corresponding real samples of wind power are sent to the GAN discriminative model, and then the wind power prediction results can be obtained with semi-supervised regression;

Step 3: The errors of each layer in the discriminative model can be obtained using Eq. (6)-(8), and the parameters of discriminative model are updated with the following formula:

$$\boldsymbol{w}_i = \boldsymbol{w}_{i-1} - \alpha_i \boldsymbol{m}_i \Big/ \left(\sqrt{\boldsymbol{v}_i} + \varepsilon\right) \tag{9}$$

$$\boldsymbol{b}_i = \boldsymbol{b}_{i-1} - \alpha_i \boldsymbol{m}_i \Big/ \left(\sqrt{\boldsymbol{v}_i} + \varepsilon\right) \tag{10}$$

where, subscript i indicates the number of iterations; $\boldsymbol{w_i}$ and $\boldsymbol{b_i}$ represent the weight vector and bias vector, respectively; $\boldsymbol{m_i}$ and $\boldsymbol{v_i}$ represent first-order and second-order moment estimation vectors; α_i is the learning rate and ε is a parameter used to prevent denominator from being equal to zero. In each iteration, $\boldsymbol{m_i}$, $\boldsymbol{v_i}$ and α_i can be updated as follows:

$$\boldsymbol{m}_i = \beta_1 \boldsymbol{m}_{i-1} + \left(1-\beta_1\right) \cdot \partial L_i / \partial \boldsymbol{w}_i \tag{11}$$

$$\boldsymbol{v}_i = \beta_2 \boldsymbol{v}_{i-1} + \left(1-\beta_2\right) \cdot \left(\partial L_i / \partial \boldsymbol{w}_i\right)^2 \tag{12}$$

$$\alpha_i = \alpha_0 \cdot \sqrt{1-\left(\beta_2\right)^i} \Big/ \left[1-\left(\beta_1\right)^i\right] \tag{13}$$

where β_1 and β_2 represent two parameters of exponential decay rate and their values are respectively set to 0.9 and 0.999; The initial learning rate α_0 is set to 10^{-3}, and then the parameter α_i can be online adjusted with the increased number of iterations;

Step 4: Given a GAN discriminative model, the regression errors are estimated and back-propagated to the generative model so that the parameters of generative model can be updated once;

Step 5: Collect the next batch of training samples and repeat Steps 1-4 until all raw training samples of wind power are traversed once;

Step 6: If the number of iterations reaches the preset value or the prediction errors is less than a certain threshold, the alternative training process should be ended at once. Otherwise, repeat Steps 1-5 once again to update the model parameters of GAN.

It can be found from algorithm analysis that the distribution of virtual samples from the generative model is closer to the statistical distribution of real wind power samples, which helps the discriminative model to find its global optimal state. Meanwhile, the regression errors evaluated from the discriminative

model can reversely update the algorithm parameters of the generative model. The GAN generative and discriminative models are alternatively optimized to achieve a Nash equilibrium in a semi-supervised manner. Consequently, the point prediction results of short-term wind power based on the GAN can be obtained.

4 Multi-Step Self-Tuning Strategy for Wind Power Ramp Event Forecasting

Wind power ramp events are generally characterized by rapid and sharp fluctuations in wind power. Due to the high and sudden rate of power change within a short period of time, the REF problem of wind power is a substantially challenging issue [8]. Here, the wind power ramp rate can be defined as follows:

$$S_r = \frac{P_{t_{\text{end}}} - P_{t_0}}{t_{\text{end}} - t_0} \tag{14}$$

where $t_{\text{end}} - t_0$ represents a given time interval and is set to 60 min in this study; P_{t_0} and $P_{t_{\text{end}}}$ denote the wind power outputs at time t_0 and t_{end}; S_r is the ramp rate in a time interval, and is considered to be a ramp event when it is larger than a given threshold. The wind power ramp forecasting plays an important role in the energy management and dispatch of modern power systems with high wind energy penetration. In this paper, based on the proposed semi-supervised learning driven GAN algorithm for wind power forecasting in Section 3, a multi-label classifier is designed for different types of wind power ramp events to facilitate the REF performance of wind power.

4.1 Self-Tuning Forecasting Strategy with Rolling Horizon Procedures

Traditional multi-step forecasting strategies utilize the forecasted results at the prior time, instead of actual wind power values, to implement a point prediction at the future time. These strategies would lead to accumulative forecasting errors and the deteriorated performance with the forward horizons [22]],[[28]. In this paper, a self-tuning REF strategy with rolling horizon procedures is proposed to utilize the updated real-time data of wind power for tuning the ramp rate of the predicted ramp events in a rolling horizon mode. This strategy can effectively improve the REF prediction accuracy without missing any ramp event spanning two adjacent time intervals. The proposed method can be described as follows:

Step 1: Implement the GAN-based WPF approach recursively to forecast wind power outputs every Δt over a forecasting horizon $[t_0, t_{\text{end}}]$ based on historical data;

Step 2: Calculate the initial wind power ramp rate S_r with Eq. (14). If the initial ramp rate is close to the pre-defined thresholds, the rolling horizon strategy is activated to tune and modify the REF results in each rolling step and set $t = t_0$;

Step 3: Input the updated real-time data of wind power at current time t for the self-tuning REF

model;

Step 4: Based on the updated real-time wind power outputs, perform the semi-supervised GAN to tune and forecast the wind power from the next time $t+\Delta t$ to the end of the rolling horizon by multi-step recursive prediction processes;

Step 5: Calculate and update the ramp power rate according to the forecasted wind power with Eq. (14) in the rolling horizon;

Step 6: Set $t = t + \Delta t$; If t is equal to t_{end}, then output the wind power ramp rate during this time interval for further REF classification; otherwise return to Step 3.

In each rolling step, the forecasted wind power and the corresponding ramp rate can be tuned and updated based on the real-time wind power observation and its variation trend. Thus, the proposed self-tuning forecasting strategy can track the fluctuation of wind power in real time and adaptively tune the REF forecasting results. The flowchart of the proposed self-tuning strategy is shown in Fig. 5.

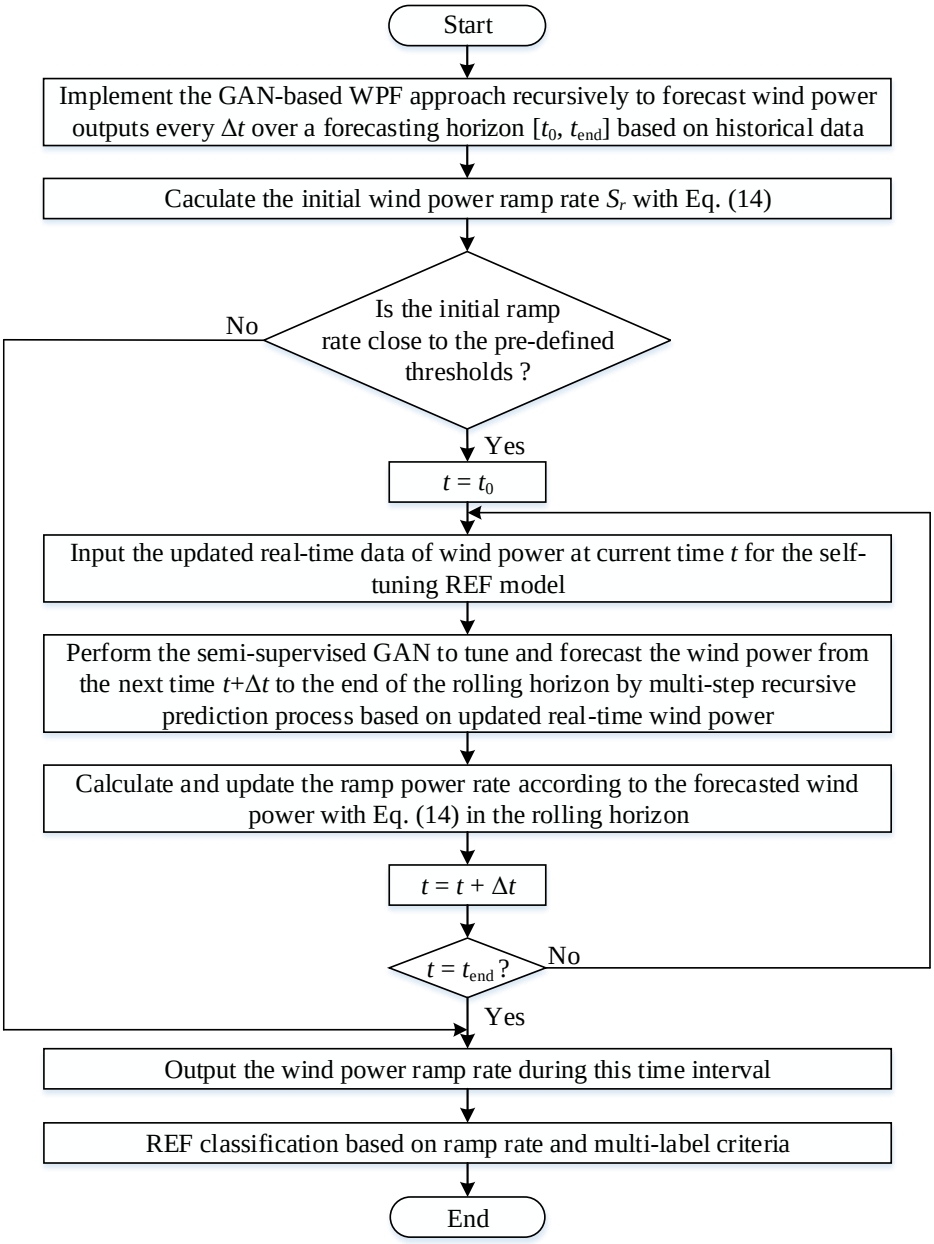

Fig. 5 The flowchart of the proposed with self-tuning REF method

4.2 Multi-Label Classifier for Ramp Events

Different types of wind power ramp events, such as ramp-up and ramp-down events with different ramp rates, have different impacts on the stability and economic operation of the smart grid [31]. In general, wind power ramp event prediction can be formulated as a multi-label classification problem. In this paper, the wind power ramp events are divided into five categories for semi-supervised learning, including large ramp up events, small ramp up events, large ramp down events, small ramp down events and no ramp events. The multi-label criteria of REF classification are listed in Table 1. Here, R_1 and R_2 are the thresholds of power ramp rates, and their values depend on the maximum installed capacity of the wind farm [33].

Table 1 Multi-label criteria of REF classification

Label of wind power ramp events	Classification criteria
Large ramp up events	$S_r > R_2$
Small ramp up events	$R_1 < S_r < R_2$
No ramp events	$-R_1 < S_r < R_1$
Small ramp down events	$-R_2 < S_r < -R_1$
Large ramp down events	$S_r < -R_2$

5 Implementation of Proposed Forecasting Method

In this paper, a hybrid prediction model based on semi-supervised regression, CNN and GAN is proposed for the forecasting of wind power and its ramp events. The proposed method combines various techniques such as data augmentation, feature extraction, and alternative training. In summary, the overall forecasting framework of the proposed prediction method is illustrated in Fig. 6.

Firstly, the VMD is applied to decompose the original time series of wind power into multiple IMF signals and one residual sub-series. Then, a random noise vector is generated and also converted into a virtual sample by the GAN generative model. This virtual sample increases the diversity for training GAN discriminative model. Subsequently, the virtual samples and IMF sub-series are taken as the inputs into the discriminative model with three convolution layers and one regression layer. Thus, the WPF results of each sub-series and its prediction errors can be obtained. Furthermore, the prediction errors are fed back to the GAN generative model to update the generative parameters, and each IMF sub-series with the residual signal correspond to an independent discriminative model. The entire WPF prediction model is trained using the alternative training process as illustrated in Section 3.4. After the GAN training

process is completed, the prediction performance for the forecasting of wind power and its ramp events can be evaluated by statistical indices.

Compared with the previous WPF and REF models, the proposed semi-supervised learning driven GAN method possesses the following advantages: (1) The GAN used in the proposed prediction method is essentially a general framework and can be combined with other time-series forecasting model with strong compatibility; (2) The proposed prediction method uses the GAN generative model to generate virtual samples for extending the set of training samples, and it can improve the prediction robustness against random noise; (3) The CNN adopted in the discriminative model has better capability for extracting time series features. Hence, these advantages can effectively improve the prediction stability, robustness and forecasting accuracy of the proposed GAN-based WPF method.

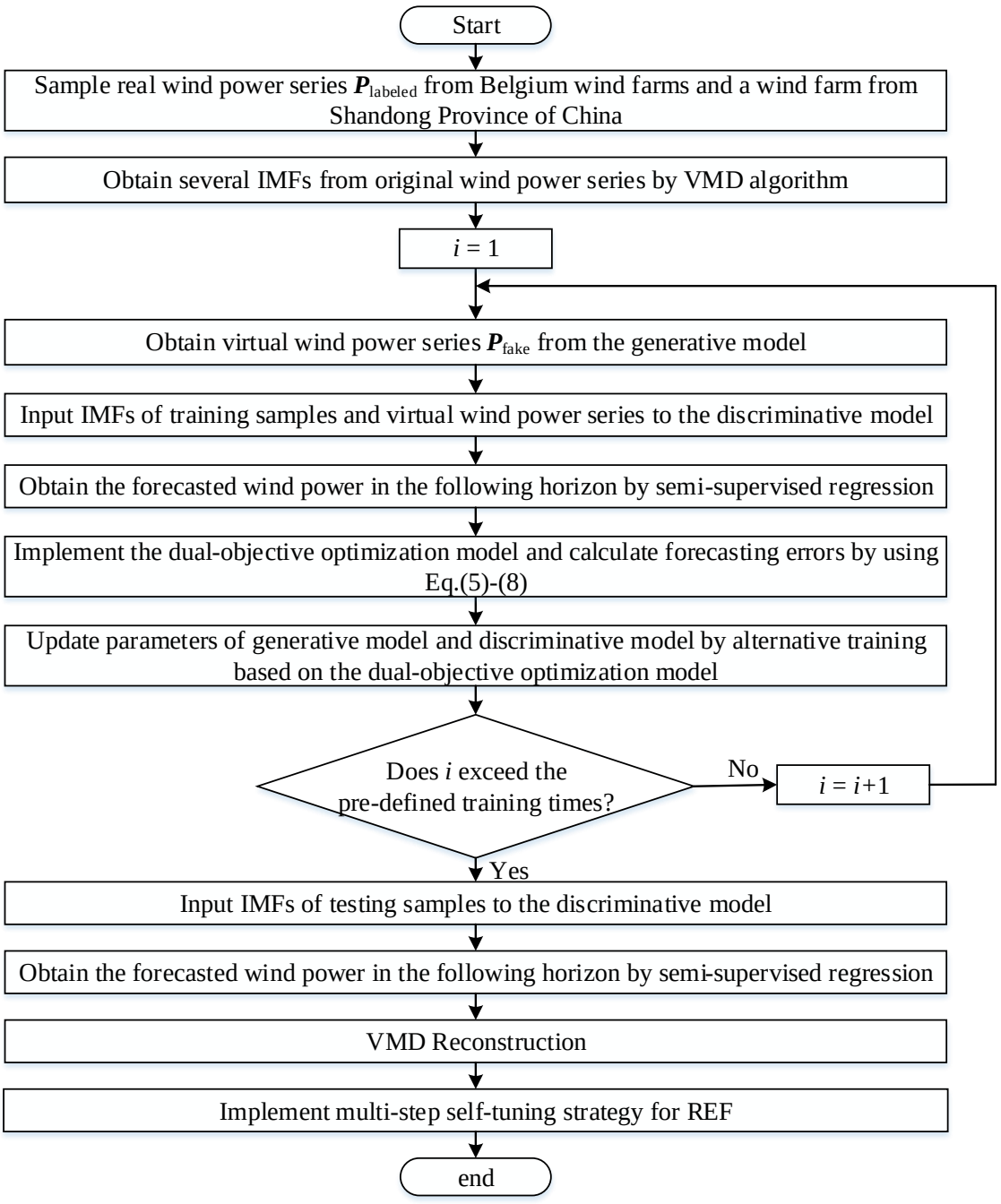

Fig. 6 Implementation framework of the proposed method

6 Evaluation Criteria

6.1 Wind Power Forecasting Metrics

In this paper, three metrics, including mean absolute error (MAE), mean absolute percentage error (MAPE) and root mean square error (RMSE), are used for evaluating the WPF performance [4]. MAE and RMSE is to assess the forecasting capacity and accuracy of the proposed prediction method, while MAPE is used to evaluate the relative deviation of point forecasting results from real wind power outputs, as follows,

$$\mathrm{MAE} = \frac{1}{N}\sum_{i=1}^{N}\left|P_i^F - P_i^R\right| \tag{15}$$

$$\mathrm{MAPE} = \frac{1}{N}\sum_{i=1}^{N}\frac{\left|P_i^F - P_i^R\right|}{P_i^R}\times 100\% \tag{16}$$

$$\mathrm{RMSE} = \sqrt{\frac{1}{N}\sum_{i=1}^{N}(P_i^F - P_i^R)^2} \tag{17}$$

where P_i^F and P_i^R represent the WPF results and the real data of wind power at the time step t_i; N denotes the total number of samples.

6.2 Ramp Event forecasting Metrics

Here, the forecast accuracy (FA) and ramp capture (RC) are chosen as evaluation indices for REF performance evaluation [7]. FA is applied to evaluate the forecasting accuracy of the proposed method, and RC is to measure the forecasting recall of the proposed method, as follows,

$$\mathrm{FA} = \frac{\mathrm{TF}}{\mathrm{TF+FF}}\times 100\% \tag{18}$$

$$\mathrm{RC} = \frac{\mathrm{TF}}{\mathrm{TF+MR}}\times 100\% \tag{19}$$

where, True Forecast (TF) represents the observed ramp events that have been predicted; False Forecast (FF) represents the unobserved ramp events that have been predicted by REF methods; Missed Ramp (MR) represents the observed ramp events ignored by REF methods.

7 Case Studies

In this case study, the proposed method has been comprehensively tested on wind power datasets from three wind farms. The real measurement from Belgium wind farms (15 min) and a wind farm from

Shandong Province of China (60 min) in 2018 are adopted to demonstrate the superiority of the proposed method on WPF and REF problems. Cases 1 and 2 adopt the real power from Wallonia and Vlaanderen wind farms for one-step ahead WPF and REF with a data resolution of 15 minutes [27], while Case 3 uses the real power from a wind farm of Shandong Province of China for multi-step ahead WPF with a data resolution of 60 minutes [5]. The wind power at the next time is forecasted based on 9 consecutive historical values of these time series, and the ratio of the number of training samples to test samples is set to 4:1 [28]. WPF and REF performance of the proposed forecasting method is compared with various algorithms including ARIMA [11], SVM [18], shallow ANN [19], CNN [27], RNN [25], ELM [22]-[23], RVFLN [24], DBN [28] and hybrid method DBN+WT.

7.1 Wind Power Forecasting

(1) Case 1

Two small datasets are adopted to test the forecasting results of the proposed prediction method. The first wind power dataset was from the Wallonia wind farm in Belgium, which has a maximum wind power output of 700.2 MW in February and 806.11 MW in August [5]. The dataset contains 1000 samples, of which 800 are training samples and 200 are testing samples. The forecasting results with the proposed method and other algorithms are shown in Fig. 7, and the statistical indices of these 200 test samples are shown in Fig. 8.

It can be found from Fig. 7 that the prediction results of the GAN-based method have very similar variation trends to the real wind power data, and the proposed forecasting method has good adaptability and flexibility. It can be clearly seen from Fig. 8 that the MAE, MAPE, and RMSE results of the proposed method are 2.9474 MW, 1.02%, and 4.0502 MW, respectively, with the best forecasting performance among all the comparative algorithms. In addition, the MAE, MAPE and RMSE of the statistical ARIMA method are 29.3359 MW, 10.28% and 34.1086MW, respectively. It can also be observed that ARIMA is not good at handling wind power data with high randomness, while RNN has relatively good performance due to its strong time-series processing capability. The improvements of MAPE results with the proposed method are 62.91% and 65.31% compared to ELM and RVFLN, respectively. Furthermore, the MAE, MAPE, and RMSE of DBN are 15.4123 MW, 5.34%, and 19.1470 MW, respectively. Obviously, the prediction performance of DBN is not as good as the results of the proposed method. This is because the size of this dataset is too small for the DBN to learn the intrinsic characteristics of wind power time series, even if WT is used. Undoubtedly, the GAN-based prediction method greatly outperforms other existing methods in all three evaluation metrics.

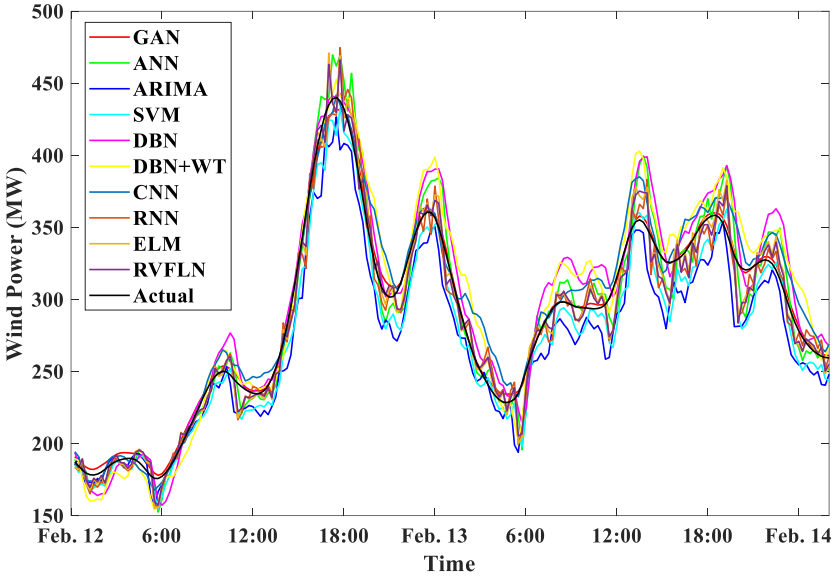

Fig. 7 WPF results on February 12-14, 2018 at Wallonia

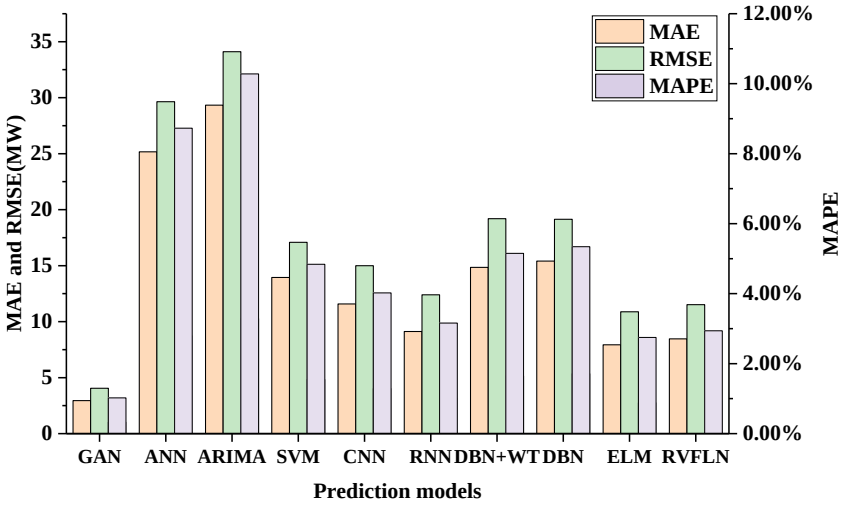

Fig. 8 WPF indices on February 12-14, 2018 at Wallonia

The second dataset is also collected from the Wallonia wind farm in Belgium. It covers the wind power data from August 3, 2018 to August 13, 2018. Similarly, the dataset contains 1000 samples, of which 200 are testing samples and the rest are training samples. The final forecasting results are shown in Fig. 9, and the statistical performance indices are given in Fig. 10. As seen from Figs. 9-10, the results of MAE, MAPE and RMSE using the GAN-based method are 1.8257 MW, 1.82%, and 2.1646 MW, respectively. The reductions on MAPE are 74.47% and 76.11% compared to ELM and RVFLN, and range from 76.36% to 88.08% compared to other methods. During the period from 10:00 to 14:00 on Aug. 3, the performance of other methods is worse than that of the proposed method. It is worth mentioning that the DBN performs the worst with the MAE, MAPE and RMSE of 15.3304 MW, 15.27% and 19.0301 MW, respectively. This is mainly because the sample size is too small so that its feature extraction capability is hugely limited. Also, the number of deep learning layers is large, which tends to cause over-fitting problem. The additional experimental performance in spring and autumn are presented in Table 2

to further validate the forecasting ability of proposed method. It can be found from Table 2 that, compared with other methods, the improvements of MAPE range from 51.82% to 78.35% with an average of 65.08% in spring, and range from 61.48% to 84.53% with an average of 73.18% in autumn. The results can be explained that wind power time-series in autumn is more irregular and unpredictable and other methods cannot extract the inherent features in wind power. Obviously, the proposed GAN is suitable for wind power forecasting with small/big sample size.

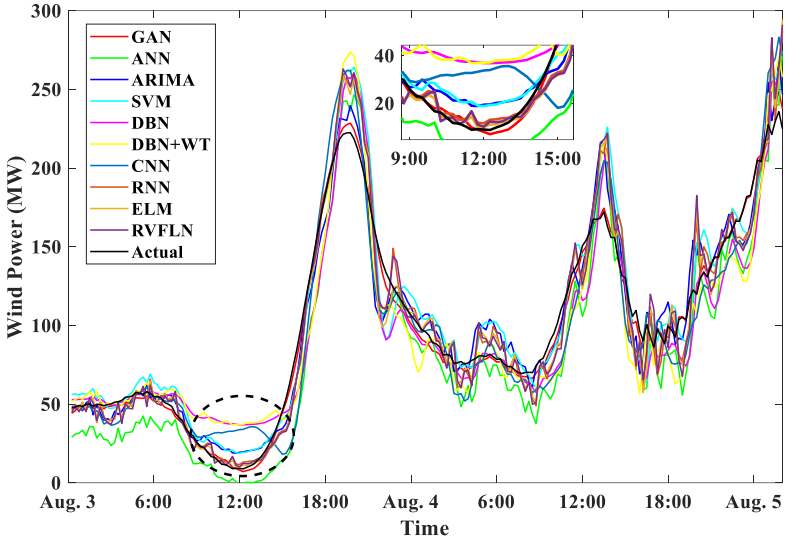

Fig. 9 WPF results on August 3-5, 2018 at Wallonia

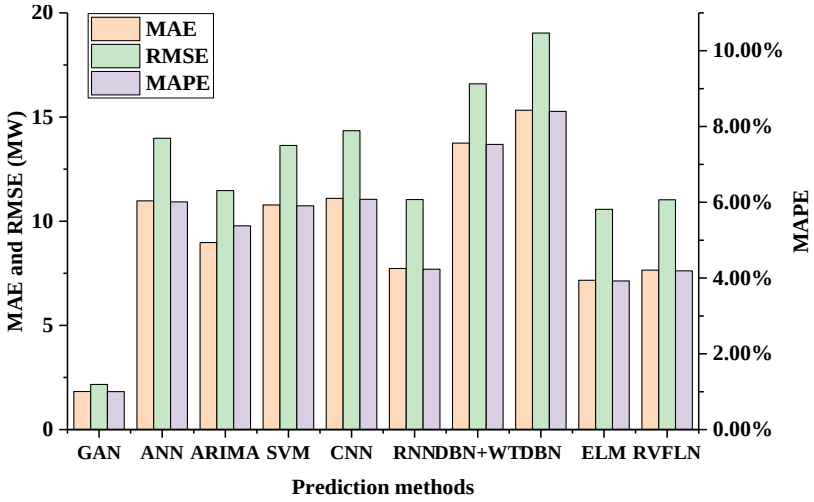

Fig. 10 WPF indices on August 3-5, 2018 at Wallonia

Table 2 WPF indices in spring and autumn of 2018 at Wallonia

Season	Index	**GAN**	ANN	ARIMA	SVM	CNN	RNN	DBN+WT	DBN	ELM	RVFLN
Spring	MAE	**3.8395**	16.5011	22.3638	8.0432	12.7801	7.9516	15.3667	18.7539	7.7709	8.0094
	RMSE	**4.8748**	20.3967	25.9973	13.2325	16.6721	12.5526	19.7234	20.8841	11.0880	13.3955
	MAPE	**1.67%**	6.38%	9.10%	4.14%	6.58%	4.09%	6.54%	7.98%	4.00%	4.52%
Autumn	MAE	**2.2173**	8.3021	6.2576	5.5050	12.7145	5.7166	9.4011	13.7104	5.5230	6.3722
	RMSE	**3.1574**	11.8202	10.1917	9.4693	16.8322	9.9971	13.5263	18.1034	9.5609	10.8962
	MAPE	**1.93%**	8.42%	6.75%	5.79%	13.37%	6.01%	9.88%	14.42%	5.81%	6.70%

(2) Case 2

This case adopts the wind power dataset from Vlaanderen in Belgium, which has a maximum wind power output of 2621.924 MW in February and 3003.185 MW in August [5], to further verify the effectiveness of the proposed forecasting method. Similar to Case 1, the dataset contains 1000 samples and covers the time period of February 12-22, 2018 and the time period of August 4 to 14, 2018. The ratio of the testing samples to the training samples is set to 1/4. The forecasting results of the GAN-based forecasting method are graphically presented in Figs.11-12. It is clear that the wind power dataset from Vlaanderen is more chaotic, with more spikes and fluctuations. While, the forecasting curve of the proposed method and the real wind power data are almost overlapped. Fig. 12 shows that, in terms of MAPE, the improvements of the proposed method range from 68.41% to 85.17% compared to other methods. During the period from 17:00 to 23:00 on Aug. 4, the proposed GAN method has small errors and low fluctuations. The 12 monthly forecasting performance in 2018 at Vlaanderen is presented in Table 3. Apparently, the MAPE of GAN varies from 0.72% to 2.74% with an average of 1.73%, which shows larger differences and stronger stability compared to other methods. From Fig. 12, it can be found that the proposed method has a slightly worse fitting degree in August than that in February. This is because wind power dataset in August is more stochastic than that in February.

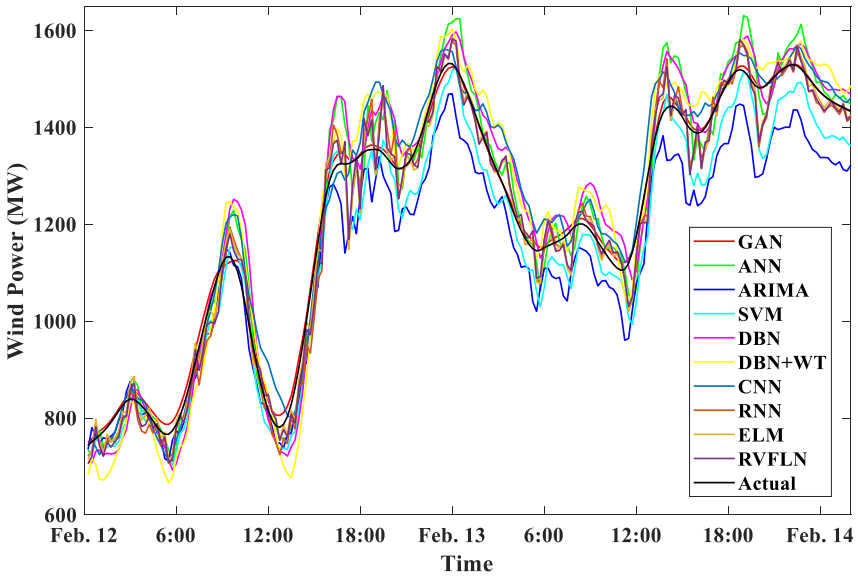

Fig. 11 WPF results on February 12-14, 2018 at Vlaanderen

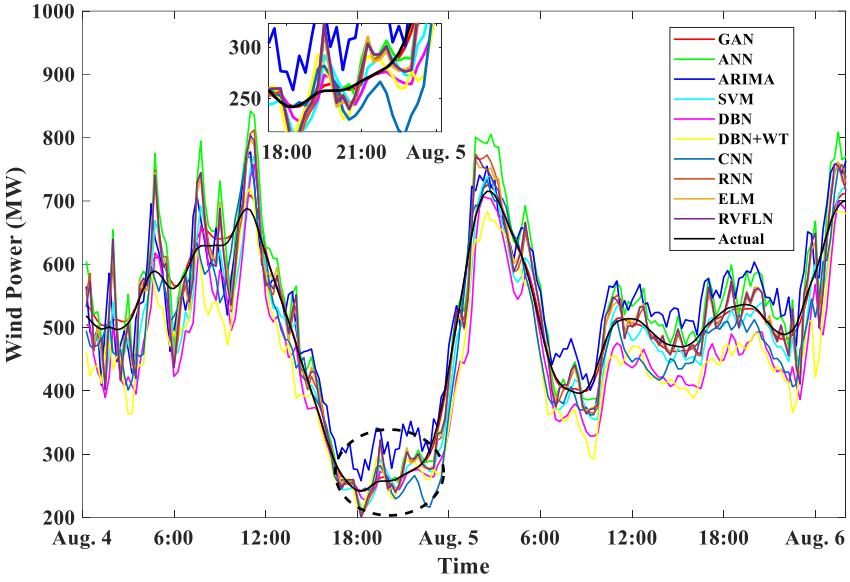

Fig. 12 WPF results on August 4-6, 2018 at Vlaanderen

Table 3 Comparative WPF indices in 2018 at Vlaanderen

Month	Index	**GAN**	ANN	ARIMA	SVM	CNN	RNN	DBN+WT	DBN	ELM	RVFLN
	MAE	**3.4521**	11.4752	11.1070	10.9442	16.2625	11.4545	18.0258	24.1351	11.0810	12.4857
Jan.	RMSE	**5.2478**	16.5239	12.6189	15.9942	24.7028	20.2510	23.2287	29.5567	16.0831	16.8384
	MAPE	**1.22%**	4.05%	3.92%	3.86%	5.74%	4.05%	6.36%	8.51%	3.91%	4.40%
	MAE	**5.0006**	27.6192	90.1810	22.8374	39.0018	23.7065	37.4699	40.2722	22.7746	28.2572
Feb.	RMSE	**6.4073**	39.8695	174.6899	33.9657	56.3376	42.8871	45.4122	52.7891	34.1481	41.2477
	MAPE	**0.72%**	3.18%	10.74%	2.63%	4.49%	2.74%	4.16%	4.64%	2.61%	3.25%
	MAE	**3.4054**	11.5878	38.7240	10.7080	15.9549	11.2778	8.7934	20.3967	10.9200	12.7575
Mar.	RMSE	**4.0058**	16.2114	49.6524	15.5112	20.4144	19.3257	10.0325	25.8894	15.8014	16.7993
	MAPE	**1.41%**	4.79%	14.28%	4.43%	6.60%	4.64%	3.64%	8.43%	4.52%	5.28%
	MAE	**3.1803**	10.9700	20.0691	9.6044	16.6270	9.7173	15.3754	21.1516	9.6368	12.9410
Apr.	RMSE	**3.9895**	15.7949	24.1794	14.9844	21.385	15.0032	17.3855	26.2702	15.0005	17.3472
	MAPE	**1.96%**	6.77%	12.89%	5.93%	10.26%	5.96%	9.89%	13.05%	5.95%	7.98%
	MAE	**2.7632**	8.3994	16.6116	7.1848	13.4779	7.6984	12.1948	18.5197	7.2062	8.5605
May.	RMSE	**3.2416**	12.0798	21.5450	11.3426	17.4205	19.0724	16.0490	23.3816	11.3553	12.3126
	MAPE	**2.04%**	6.21%	10.25%	5.31%	9.97%	5.66%	8.61%	13.70%	5.33%	6.33%
	MAE	**1.7654**	7.2302	19.0616	5.9461	12.1849	6.2680	13.0272	15.9288	6.0291	8.2463
Jun.	RMSE	**2.4162**	9.9705	20.4323	9.0357	15.9454	9.2167	15.7521	20.1558	9.0885	10.7411
	MAPE	**1.29%**	5.30%	13.97%	4.36%	8.93%	4.59%	9.55%	11.67%	4.42%	6.04%
	MAE	**1.3639**	7.3552	14.9137	5.6382	11.9737	5.9759	8.5062	15.5843	5.7813	8.3589
Jul.	RMSE	**1.8084**	9.9744	18.3835	9.0717	15.2494	10.8305	11.3459	19.7724	9.1003	10.8683
	MAPE	**1.16%**	6.25%	12.78%	4.79%	10.17%	5.04%	7.66%	13.24%	4.91%	7.10%
	MAE	**7.7139**	27.0173	85.8003	23.5467	39.9314	23.5441	21.9100	44.2481	22.3807	28.9852
Aug.	RMSE	**20.7972**	46.2334	96.9450	41.5225	63.6969	41.2537	30.1810	66.5978	36.0501	48.5520
	MAPE	**1.44%**	5.02%	15.96%	4.38%	7.43%	4.39%	4.07%	8.23%	4.15%	5.39%
	MAE	**4.7658**	9.7171	26.9542	7.8288	14.0106	7.9354	11.5627	22.1869	7.9368	7.9066
Sept.	RMSE	**5.6984**	14.1535	33.4521	12.9691	19.4105	13.1058	13.9201	29.7170	13.1495	13.0896
	MAPE	**2.74%**	5.59%	15.67%	4.50%	8.06%	4.55%	6.65%	12.76%	4.57%	4.55%
	MAE	**3.5025**	9.8866	16.5179	8.2902	14.0612	8.4080	12.4085	23.3892	8.1528	9.4537
Oct.	RMSE	**4.1277**	13.5258	21.3361	12.5897	18.4658	12.7464	16.9578	29.2207	12.1510	12.9309
	MAPE	**2.09%**	5.90%	9.51%	4.94%	8.39%	5.00%	7.69%	13.95%	4.82%	5.64%

Nov.	MAE	**3.5297**	11.2897	13.4987	9.8082	15.1153	9.9691	10.7995	25.7856	9.8285	9.9583
	RMSE	**4.5279**	15.6792	18.8425	14.6805	19.6832	15.1437	13.4643	32.3875	14.7513	14.8678
	MAPE	**1.77%**	5.68%	6.79%	4.93%	7.60%	5.01%	5.43%	12.96%	4.94%	5.01%
Dec.	MAE	**4.1139**	12.5960	30.1345	11.0630	16.3319	11.4216	15.2927	29.1251	13.1970	13.5654
	RMSE	**4.9410**	17.1936	36.6183	16.2606	21.2684	17.6006	19.3318	35.5000	17.4049	17.5322
	MAPE	**1.43%**	4.39%	10.50%	3.85%	5.69%	3.98%	5.33%	10.15%	4.90%	4.73%

(3) Case 3

This case adopts the real data of a wind farm from Shandong Province of China to verify the overall forecasting performance of the proposed method on one-step prediction and multi-step prediction tasks. The multi-step forecasting is an iterative point prediction process and performed in a rolling mode with high forecasting accuracy [30]. In each iteration, the one-step prediction results in the prior time steps are used as the inputs of multi-step forecasting for a certain time point. The forecasting structure and parameter settings are the same as that in the previous Cases 1-2. The one-step prediction and the multi-step prediction results are illustrated in Figs. 13-14, respectively. The corresponding statistical indices of benchmarking algorithms are given in Tables 4-5. In Table 4, the MAE, MAPE and RMSE indices of the proposed method are 0.3154 MW, 2.55% and 0.4326 MW, respectively. In Table 5, the MAE, MAPE, and RMSE of the proposed method are 0.5944 MW, 4.80%, and 0.8349 MW, respectively. The prediction results from Figs. 13-14 and Tables 4-5 show that the GAN-based prediction method can be used in the multi-step wind power prediction tasks.

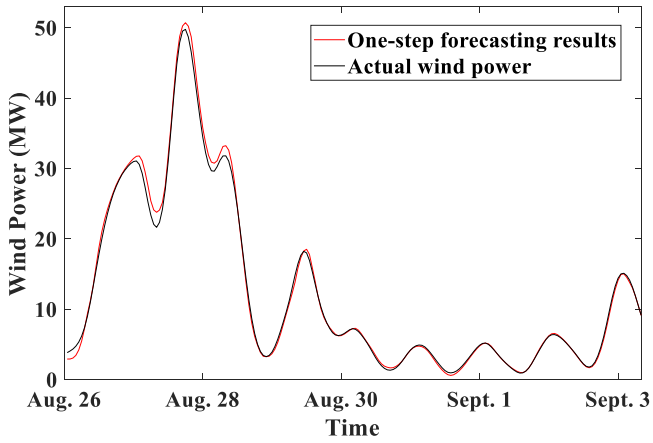

Fig. 13 One-step WPF results of the proposed approach

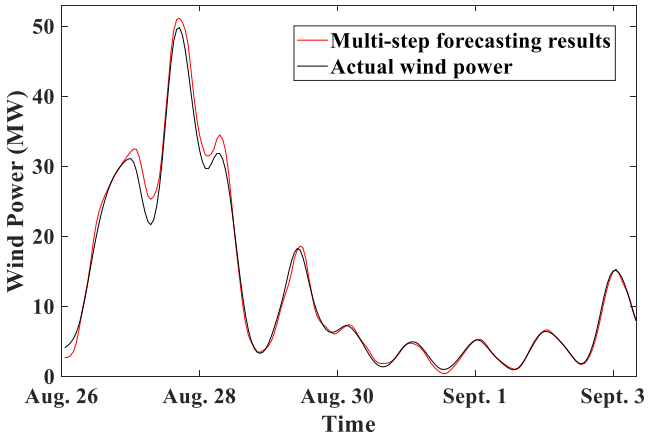

Fig. 14 Multi-step WPF results of the proposed approach

Table 4 One-step WPF indices with different forecasting methods

Index	**GAN**	ANN	ARIMA	SVM	CNN	RNN	DBN+WT	DBN	ELM	RVLFN
MAE	**0.3154**	1.0914	2.2214	1.3016	1.1451	0.9557	1.6569	1.7766	1.1167	1.0435
RMSE	**0.4326**	1.7085	3.3249	2.0817	1.8677	1.3084	2.2684	2.5587	1.7794	1.6505
MAPE	**2.55%**	9.61%	19.56%	11.46%	10.08%	8.41%	14.59%	16.94%	9.78%	9.19%

Table 5 Multi-step WPF indices with different forecasting methods

Index	**GAN**	ANN	ARIMA	SVM	CNN	RNN	DBN+WT	DBN	ELM	RVLFN
MAE	**0.5944**	2.0999	2.5458	2.2935	1.6997	1.5696	1.8653	2.3543	2.2236	2.1674
RMSE	**0.8349**	3.1431	3.9001	3.4389	2.7043	2.3450	2.8867	3.5232	3.3483	3.2750
MAPE	**4.80%**	18.46%	22.37%	20.16%	16.30%	14.04%	17.68%	20.74%	19.47%	18.14%

A comparison of the calculation time with all the forecasting methods is presented in Table 6. All the methods are implemented in MATLAB R2018b and carried out on a personal computer with 2.60GHz Intel CPU and 8 GB of RAM. The dataset contains 800 training samples and 200 testing samples. From Table 6, it can be seen that the proposed GAN takes more time for forecasting than ARIMA, SVM, RNN, shallow ANN, CNN, ELM, and RVFLN. That is because the proposed method employs the VMD for signal decomposition, and both generative and discriminative models need to be trained. In addition, the calculation time of the GAN-based prediction algorithm is shorter than that of DBN-based forecasting algorithm. This can be explained by the fact that the DBN has a complicated training process including layer-wise training and fine-tuning. Consequently, it can be seen that the proposed prediction algorithm based on GAN is attractive from the aspects of prediction performance and efficiency.

Table 6 Computational time of ten prediction method

	GAN	ANN	ARIMA	SVM	CNN	RNN	DBN+WT	DBN	ELM	RVFLN
Runtime/s	**17.9208**	12.3658	5.6708	4.5185	10.9633	5.9640	32.2438	21.3253	11.5306	13.7885

7.2 Ramp Event Forecasting of Wind Power

This section aims to test the overall performance of the self-tuning GAN-based method for the REF problem of wind power. The multi-label classifier is used to identify different types of power ramp events including LU (large ramp up), SU (small ramp up), NO (no ramp), SD (small ramp down) and LD (large ramp down). The threshold values of ramp rate R_1 and R_2 correspond to 5% and 10% of the installed wind power capacity, and the leading time is set to 60 min. The ramp rate curves obtained from pure REF and self-tuning REF are shown in Figs. 15-16. It can be seen that the proposed self-tuning REF method can successfully predict most of observed events. For example, in Fig. 15, a LU is predicted by self-tuning REF. While, this LU is not detected by pure REF at 15:00 on Feb. 12. The undetected ramp event using pure REF method also happens at 22:00 on Feb. 12. They are marked with black circles. At 1:00 AM on Feb. 13, the SD with a red circle is predicted by pure REF, but the prediction result lags behind actual ramp event, which is useless for real-time scheduling. In Fig. 16, a similar situation can also be found at 21:00 on Aug. 3.

The statistical forecasting performance are presented in Tables 7-8, respectively. The TF and FF indices can indicate the number of observed/unobserved ramp events of wind power predicted by different algorithms. In general, the larger values of FA and RC denote the better algorithm performance.

From Table 7, the proposed GAN successfully captures 1 large ramp up event, 7 small ramp up events, 6 small ramp down events and 1 large ramp down events, and thus the index TF is equal to 15 (1+7+6+1=15), while the FF is equal to 0. The FA calculated by Eq. (18) is equal to 100%. On the other hand, there is 1 small ramp down event which is not captured by the proposed method, and the MR is 0. Thus the RC is equal to 93.75%. Comparatively, for the hybrid method DBN+WT, 4 large ramp up events have been predicted, but only 1 events is actually observed. Thus, the TF is equal to 14 (1+6+7+0=14), and the FF and MR are 6 and 2, respectively. Also, although the CNN algorithm exhibits the highest FF index, there are still 2 small ramp up events and 1 large ramp down event which are not predicted by the CNN. Compared to other algorithms in Table 7, the FA from the proposed method is 100.00% with the improvement of 33.33%. The RC from the proposed method is 93.75% with the improvement of 33.33%. It can be found from Table 8 that the proposed method have successfully captured 10 small ramp up events and 2 large ramp down events, but there is 1 small ramp down event to be wrongly predicted. Compared to other algorithms in Table 8, the FA of the proposed method is 93.33% with the improvement of 34.06%. The RC of the proposed method is 100.00% with the improvement of 42.86%. It can be concluded from these results that the proposed GAN-based forecasting method can provide the superior REF performance than the existing prediction algorithms.

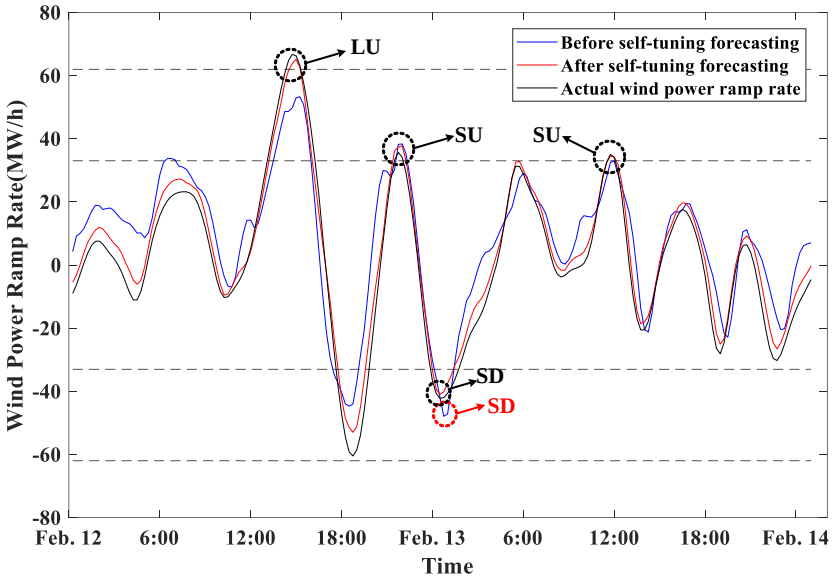

Fig. 15 REF results on February 12-14, 2018 at Wallonia

Table 7 REF indices in February 2018 at Wallonia (Total 16 ramp events)

Index	Real	**GAN**	ANN	ARIMA	SVM	CNN	RNN	DBN+WT	DBN	ELM	RVFLN
LU	1	**1**	1	0	1	1	2	4	4	1	0
SU	7	**7**	8	7	6	5	4	6	4	6	5
NO	33	**34**	32	34	34	36	36	29	34	35	34
SD	7	**6**	5	6	5	7	4	10	4	6	8
LD	1	**1**	3	2	3	0	3	0	3	1	2

FA	\	**100.00%**	82.35%	93.33%	86.67%	100.00%	76.92%	70.00%	66.67%	100%	86.67%
RC	\	**93.75%**	87.50%	87.50%	81.25%	81.25%	62.50%	87.50%	62.50%	87.50%	81.25%

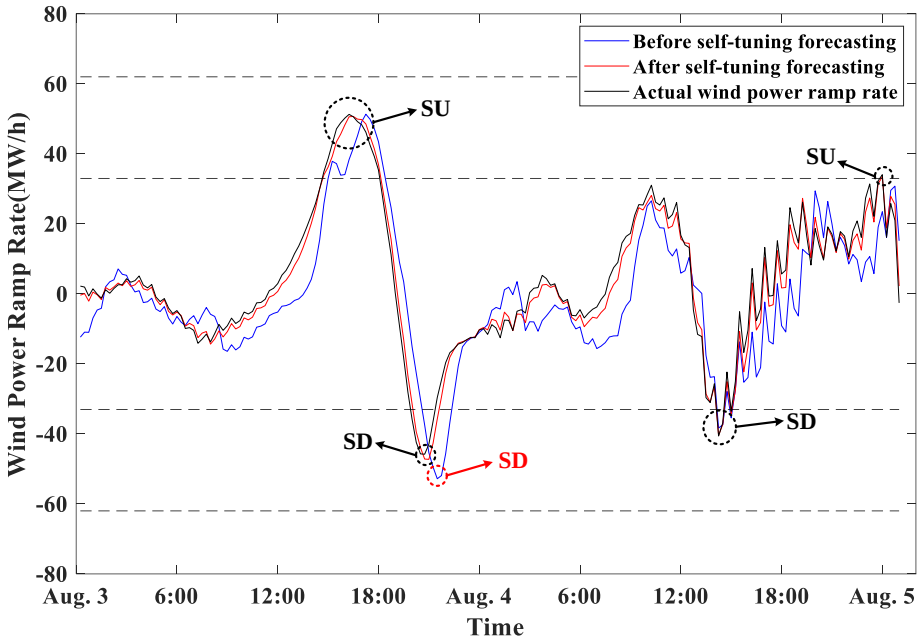

Fig. 16 REF results on August 3-5, 2018 at Wallonia

Table 8 REF indices in August 2018 at Wallonia (Total 14 ramp events)

Index	Real	**GAN**	ANN	ARIMA	SVM	CNN	RNN	DBN+WT	DBN	ELM	RVFLN
LU	0	**0**	2	1	4	3	4	4	3	0	1
SU	10	**10**	8	8	5	7	7	4	6	9	12
NO	35	**34**	33	36	36	35	33	37	36	33	32
SD	2	**3**	5	2	1	2	2	2	2	5	3
LD	2	**2**	1	2	3	2	3	2	2	2	1
FA	\	**93.33%**	68.75%	92.31%	61.54%	78.57%	68.75%	66.67%	76.92%	81.25%	76.47%
RC	\	**100.00%**	78.57%	85.71%	57.14%	78.57%	78.57%	57.14%	71.43%	92.85%	92.85%

7.3 Performance Analysis

It can be found that, compared with other benchmarking methods, the proposed method can exhibit a superior performance in term of different lengths of wind power data and prediction horizons. The highlights can be explained as follows: 1) The proposed method uses the VMD to decompose the original time-series data of wind power into IMF sub-series with smooth outer contours, and each IMF is used as the inputs to discriminative model for semi-supervised regression with label learning, thereby improving the predictability of the WPF and REF models; 2) The GAN generative model can generate extra training samples, enhancing the generalization capability of the proposed method, while traditional deep learning algorithms, like the DBN algorithm, are not suitable for the WPF problem with small size of dataset. 3) The proposed self-tuning REF strategy can dynamically adjust and modify the multi-step ramp event

parameters based on real-time information. Additionally, the ramp events can be classed by multi-label criterion, allowing dispatchers to prepare for future unknown ramp events.

Regarding the calculation time, the proposed method is not the most efficient compared with other methods. The reason can be explained that, a signal decomposition technique is employed and three independent GAN models need to be trained separately. Also, the GAN contains two deep learning networks, which double the time consumption for updating network parameters. In the near future, the on-going investigations will focus on how to improve the calculation efficiency, making the proposed method suitable for practical applications in different renewable energy forecasting problems.

8 Conclusions

In this paper, in order to alleviate the negative impact of wind power uncertainties on the forecasting accuracy, a hybrid prediction model combining multi-step self-tuning strategy and semi-supervised GAN with generative and discriminative models is developed for the WPF and REF problems. The proposed method has been comprehensively tested and compared with statistical method, classical neural networks and deep learning algorithms, using wind power time series collected from real wind farms. From these obtained forecasting results, it is observed that the proposed method can outperform all the benchmarking algorithms in terms of various evaluation metrics. Statistically, compared to other methods at Wallonia wind farm, the highest improvements of MAE, RMSE and MAPE are 89.95%, 88.64%, and 88.08%, respectively. Also, the highest improvements of MAE, RMSE, and MAPE are 87.58%, 87.86%, and 84.48% at Vlaanderen wind farm, respectively. Moreover, it has been proved in Case 3 that the proposed multi-step self-tuning REF strategy is efficient and effective to improve the wind power ramp event prediction accuracy on the start time of ramp, duration and ramp rate. These statistical results demonstrate the superior performance of the proposed method, showing that it has a great potential for future applications in smart grid.

Acknowledgment

This work was jointly supported by the Research Grants Council of the HKSAR Government (Grant No. R5020-18), the Innovation and Technology Commission of the HKSAR Government to the Hong Kong Branch of National Rail Transit Electrification and Automation Engineering Technology Research Center (Grant No. K-BBY1), the National Natural Science Foundation of China (51877072), and Huxiang Young Talents programme of Hunan Province under Grant 2019RS2018.

References

[1] Huaizhi Wang, Yangyang Liu, Bin Zhou, Canbing Li, Guangzhong Cao, Nikolai Voropai, Evgeny Barakhtenko, Taxonomy research of artificial intelligence for deterministic solar power forecasting, Energy Conversion and Management, Volume 214, 2020, 112909.

[2] Huaizhi Wang, Zhenxing Lei, Xian Zhang, Bin Zhou, Jianchun Peng, A review of deep learning for renewable energy forecasting, Energy Conversion and Management, Volume 198, 2019, 111799.

[3] World Wind Energy statistics, Available online: https://wwindea.org/blog/2019/02/25/wind-power-capacity-worldwide-reaches-600-gw-539-gw-added-in-2018.

[4] Da Xu, Qiuwei Wu, Bin Zhou, et al. Distributed multi-energy operation of coupled electricity, heating and natural gas networks. IEEE Transactions on Sustainable Energy, DOI: 10.1109/TSTE.2019.2961432, in press, 2020.

[5] Huaizhi Wang, Gangqiang Li, Guibin Wang, Jianchun Peng, Hui Jiang, Yitao Liu, Deep learning based ensemble approach for probabilistic wind power forecasting. Applied Energy, 2017, 188: 56-70.

[6] Mingjian Cui, Jianhui Wang, Bo Chen. Flexible machine learning-based cyberattack detection using spatiotemporal patterns for distribution systems. IEEE Transactions on Smart Grid, 2020, 11(2): 1805-1808.

[7] Cristobal Gallego-Castillo, Alvaro Cuerva-Tejero, Oscar Lopez-Garcia. A review on the recent history of wind power ramp forecasting. Renewable and Sustainable Energy Reviews, 2015, 52: 1148-1157.

[8] Ferreira, C., Gama, J., Matias, L., Botterud, A., Wang, J., and INESC Porto). A survey on wind power ramp forecasting. United States: N. p., 2011. Web. DOI:10.2172/1008309.

[9] Matthias Lange and Ulrich Focken, Physical approach to short-term wind power prediction, Springer: Berlin Heidelberg, 2006.

[10] Niya Chen, Qian Zheng, Ian T. Nabney, et al. Wind power forecasts using Gaussian processes and numerical weather prediction. IEEE Transactions on Power Systems, 2014, 29(2): 656-665.

[11] Peiyuan Chen, Troels Pedersen, Birgitte Bak-Jensen, et al. ARIMA-based time series model of stochastic wind power generation. IEEE Transactions on Power Systems, 2010, 25(2): 667-676.

[12] Matti Koivisto, Janne Seppanen, Ilkka Mellin, et al. Wind speed modeling using a vector autoregressive process with a time-dependent intercept term. International Journal of Electrical Power & Energy Systems, 2016, 77: 91-99.

[13] DY Hong, TY Ji, MS Li, et al. Ultra-short-term forecast of wind speed and wind power based on morphological high frequency filter and double similarity search algorithm. International Journal of Electrical Power & Energy Systems, 2019; 104: 868-879.

[14] Corlos D. Zuluaga, Mauricio A. Álvarez, Eduardo Giraldo. Short-term wind speed prediction based on robust Kalman filtering: An experimental comparison. Applied Energy, 2015, 156: 321-330.

[15] Yun Wang, Haibo Wang, Dipti Srinivasan, Qinghua Hu. Robust functional regression for wind speed forecasting based on Sparse Bayesian learning. Renewable Energy, 2019, 132: 43-60.

[16] Shengwei Fei. A hybrid model of EMD and multiple-kernel RVR algorithm for wind speed prediction. International Journal of Electrical Power & Energy Systems, 2016, 78: 910-915.

[17] Jinliang Zhang, Yiming Wei, Zhougfu Tan. An adaptive hybrid model for short term wind speed forecasting. Energy, 2020, DOI: 10.1016/j.energy.2019.06.132.

[18] Jianwu Zeng, Wei Qiao. Short-term wind power prediction using a wavelet support vector machine. IEEE Transactions on Sustainable Energy, 2012; 3(2): 255-264.
[19] Chigbogu Godwin Ozoegwu. Artificial neural network forecast of monthly mean daily global solar radiation of selected locations based on time series and month number. Journal of Cleaner Production, 2019, 216: 1-13.
[20] Yagang Zhang, Bing Chen, Guifang Pan, Yuan Zhao. A novel hybrid model based on VMD-WT and PCA-BP-RBF neural network for short-term wind speed forecasting. Energy Conversion and Management, 2019, 195: 180-197.
[21] Dehua Zheng, Eseye Abinet Tesfaye, Jianhua Zhang, et al. Short-term wind power forecasting using a double-stage hierarchical ANFIS approach for energy management in microgrids. Protection & Control of Modern Power Systems, 2017, 2(1): 13-22.
[22] Wenlong Fu, Kai Wang, Chaoshun Li, et al. Multi-step short-term wind speed forecasting approach based on multi-scale dominant ingredient chaotic analysis, improved hybrid GWO-SCA optimization and ELM. Energy Conversion and Management, 2019, 187: 356-377.
[23] Zhi Li, Lin Ye, Yongning Zhao, et al. Short-term wind power prediction based on extreme learning machine with error correction. Protection & Control of Modern Power Systems, 2016, 1(1):1-8.
[24] Ye Ren, P.N.Suganthan, N.Srikanth, et al. Random vector functional link network for short-term electricity load demand forecasting. Information Sciences, 2016, 367: 1078-1093.
[25] Qing Cao, Ewing Bradley T, Thompson Mark A. Forecasting wind speed with recurrent neural networks. European Journal of Operational Research, 2012, 221(1): 148-154.
[26] Hui Liu, Xiwei Mi, Yanfei Li. Smart deep learning based wind speed prediction model using wavelet packet decomposition, convolutional neural network and convolutional long short term memory network. Energy Conversion and Management, 2018, 166: 120-131.
[27] Huaizhi Wang, Haiyan Yi, Jianchun Peng, Guibin Wang, Yitao Liu, Hui Jiang, Wenxin Liu. Deterministic and probabilistic forecasting of photovoltaic power. Energy Conversion and Management, 2017, 153: 409-422.
[28] Huaizhi Wang, Guibin Wang, Gangqiang Li, Jianchun Peng, Yitao Liu. Deep belief network based deterministic and probabilistic wind speed forecasting approach. Applied Energy, 2016, 182: 80-93.
[29] Hui Liu, Hongqi Tian, Chao Chen, Yanfei Li. An experimental investigation of tow Wavelet-MLP hybrid frameworks for wind speed prediction using GA and PSO optimization. International Journal of Electrical Power & Energy Systems, 2013, 52: 161-173.
[30] Tascikaraoglu, M. Uzunoglu. A review of combined approaches for prediction of short-term wind speed and power. Renewable and Sustainable Energy Reviews, 2014, 34: 243-254.
[31] Hamidreza Zareipour, Dongliang Huang, William Rosehart. Wind power ramp events classification and forecasting: A data mining approach. IEEE Power and Energy Society General Meeting, 2011, pp. 1-3.
[32] Bossavy A, Girard R, Kariniotakis G. Forecasting ramps of wind power production with numerical weather prediction ensembles. Wind Energy, 2012, 16(1): 51-63.
[33] Mingjian Cui, Deping Ke, Yunazhang Sun, et al. Wind power ramp event forecasting using a stochastic scenario generation method. IEEE Transactions on Sustainable Energy, 2015, 6(2): 422-433.
[34] Kusiak A. Prediction of Wind Farm Power Ramp Rates: A Data-Mining Approach. Journal of Solar Energy

Engineering, 2009, 131(3): 376-385.
[35] Harsh S Dhiman, Dipanka Deb, Josep M Guerrero. Hybrid machine intelligent SVR variants for wind forecasting and ramp events. Renewable and Sustainable Energy Reviews, 2019, 108: 369-379.
[36] Mingjian Cui, Yyanzhang Sun, Anthony R. Florita, B. Hodge, D. Ke, Y. Sun. An optimized swinging door algorithm for identifying wind ramping events. IEEE Transactions on Sustainable Energy, 2016, 7(1): 150-162.
[37] Goodfellow IJ, Pouget-Abadie J, Mirza M, et al. Generative adversarial nets, International Conference on Neural Information Processing Systems, Kuching, Malaysia, 2014, pp. 2672-2680.
[38] Zhangling Chen, Ce Wang, Huaming Wu, Kun Shang, Jun Wang. DMGAN: Discriminative metric-based generative adversarial networks. Knowledge-Based Systems, 2019, DOI: 10.1016/j.knosys.2019.105370.
[39] Kostopoulos G, Karlos S, Kotsiantis S, Ragos O. Semi-supervised regression: A recent review. Journal of Intelligent & Fuzzy Systems, 2018, 35(2): 1483-1500.